Physica B: Condensed Matter xxx (2017) 1–6

Contents lists available at ScienceDirect

Physica B: Condensed Matter

journal homepage: www.elsevier.com/locate/physb

Influence of the irradiation in cement for the Brazilian radioactive waste repositories: Characterization via X-ray diffraction, X-ray tomography and quasielastic neutron scattering

Eduardo Gurzoni Alvares Ferreira [a], Fabiano Yokaichiya [b], Júlio Takehiro Marumo [a], Roberto Vicente [a], Francisco Garcia-Moreno [b], Paul H. Kamm [c], Manuela Klaus [a], Margarita Russina [b], Gerrit Gunther [b], Catalina Elena Jimenez [b], Margareth K.K.D. Franco [a,*]

[a] *Instituto de Pesquisas Energéticas e Nucleares - IPEN-CNEN/SP, Brazil*
[b] *Helmholtz-Zentrum Berlin für Materialienund Energie - BERN - HZB, Germany*
[c] *Techniesche Universitat Berlin, Germany*

ARTICLE INFO

Keywords:
Portland cement
Radioactive waste
Repository
X-ray diffraction
MicroTomography
Quasielastic scattering

ABSTRACT

Powerful characterization techniques have allowed detailing the investigation of cementitious materials that must endure for millennia as an engineered barrier in radioactive waste repositories. Cement is used in the repository, as waste immobilization matrix, structural material and an additional barrier against the contact of the waste with the biosphere. The material properties have to comply with requirements in respect to a number of parameters including homogeneity, permeability, and leachability, as well as withstand mechanical stress, heat, chemical and microbial attack, and the effects of ionizing radiation.

The present study aims to investigate the behavior of cementitious materials contributing to the understanding of the processes that occur in hydrated cement under the environmental conditions of a repository and to estimate the durability of these materials. In this study was observed the changes caused by radiation, to which the material was exposed. A reference Portland cement paste and grout samples were compared with irradiated ones by X-ray diffraction and Tomography. Original and valuable results concerning the investigation of the influence of radiation on cement samples were also obtained by quasielastic scattering. These results are not accessible by others techniques.

1. Introduction

Portland cement is a typical material in the elements of a repository for radioactive waste. In this context, the Portland cement can be used as a waste immobilization matrix and structural material and plays a role as an additional engineering barrier against the scape of radionuclides from repositories. Despite this, its long-term performance is still an issue that has to be addressed in order to increase the confidence that the material will perform as required during the service life of the facility. The service life of materials in radioactive waste repositories is expected to extend from 300 years, for low-level wastes, to more than 10 thousand years for high level waste and spent nuclear fuel.

The nuclear research center “Instituto de Pesquisas Energéticas e Nucleares "(IPEN-CNEN/SP) in Brazil is developing a concept of repository for disused radioactive sources, designed as a deep borehole. In this concept, cementitious materials will be used as structural material and backfill, on which the long-term safety of the facility will largely depend.

In the repository, the cement will be exposed to several deleterious conditions that can change its mineralogical, chemical and mechanical properties. The processes that are expected to occur under repository conditions are:

1. Water penetration from the environment causing infiltration of aggressive ions into the cement paste and leaching of cement compounds, especially calcium hydroxide, and reducing the pH of the cement paste. The loss of Portlandite by leaching will increase the porosity and reduce the cohesion and mechanical resistance of the paste structure. Lower pH will reduce the passivation effect of the cement, allowing higher corrosion rates of the steel structure. Water-

* Corresponding author.
E-mail address: mkfranco@ipen.br (M.K.K.D. Franco).

https://doi.org/10.1016/j.physb.2018.01.018
Received 5 August 2017; Received in revised form 3 January 2018; Accepted 9 January 2018
Available online xxxx
0921-4526/

Table 1
Amount of the components in the grout mix.

Cement (CP II-Z)	Normalize Sand	Additive (Superflow 4000)	Distilled Water
400 g	400 g	2 g	200 g

borne aggressive ions infiltrate into the cement paste, reacting with cement compounds, changing the microstructure, increasing porosity and/or increasing the internal volume of hydrated cement phases [1–7];

2. Elevation of the temperature caused by the radiation field and the geothermal gradient at high depths [8–11];
3. Pressure gradients during the setting of the cement slurry and the service life of the facility;
4. Radiolysis of water and other compounds because of the radiation doses that cement will accumulate during the service life of the facility [12–18];
5. The natural evolution of the cement mineralogy in thousands of years changes its chemical composition and mineralogy, for instance by the reaction alkali-aggregate. The long-term hydration of the unreacted anhydrous cement compounds isolated by the layer of Calcium-Silicate-Hydrate (C—S—H) gel around cement grains in initial ages will slowly change the composition of the material.

Table 2
Results of normalized Rietveld Refinements for the two samples.

Parameters	M-NI	M-IR
GOF	2.818	4.79
Phases/Weight %		
Alite + Belite	35.66	30.3
Colville	4.03	1.25
Portlandite	26.54	32.87
Calcite	17.25	14.52
Ettringite	4.63	0.198
CSH-gel	10.18	20.85

Under irradiation, the pore water present in cement paste undergoes radiolysis and some radiolysis products are highly reactive, as electrons, hydroxyl radicals and hydrogen peroxide. These radiolysis products will interact with cement paste and its hydration products, forming a wide range of compounds and secondary reagents [12,13].

The present study aims at investigating the behavior of Portland cement grout submitted to a gamma radiation field and evaluate the radiation doses that are capable of causing changes in Portland cement mineralogy and microstructure, as well as set up a relationship between irradiation and its durability.

Portland cement grout specimens cast in laboratory were irradiated with a ^{60}Co source, located at IPEN-CNEN/SP. The specimens were submitted to different doses and the radiation effects were evaluated by X-

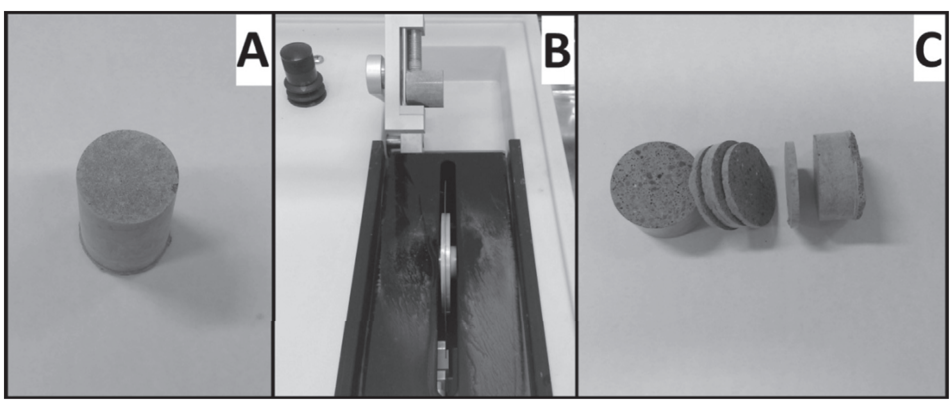

Fig. 1. Samples taken from the tray (A) and cut (B) in 2 mm slices specimens (C).

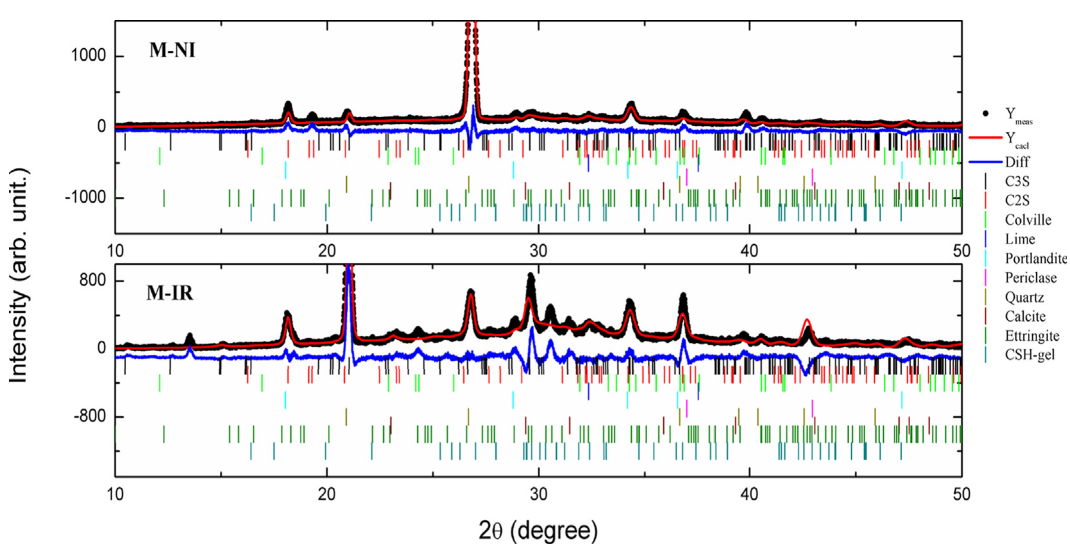

Fig. 2. Refinement of diffractogram of non-irradiated (M − NI) and irradiated (M-IR) samples. Black points are the experimental data, the red line is the calculated diffractogram and the blue line is the difference between experimental and calculated data. The bars (|) show the main peak positions of the phases. (For interpretation of the references to colour in this figure legend, the reader is referred to the Web version of this article.)

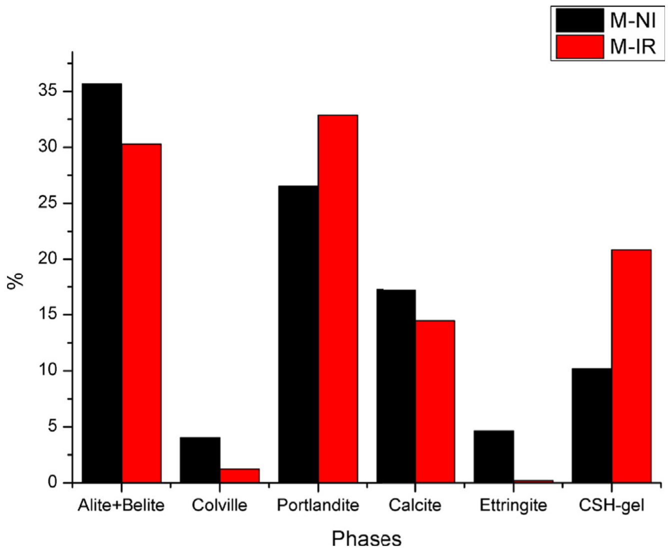

Fig. 3. Phases percentage of 2 selected samples.

Table 3
Pore volumes and pore fractions in the samples.

	M-NI	M-IR	CP
Sample volume[mm^3]	7.20	10.05	3.41
Total pore volume [mm^3]	0.43	0.79	0.03
Pore fraction [%]	6,01%	7.88%	0.92%

ray diffraction, Tomography and Time-of-Flight Spectrometer.

The results of this research will be useful in the long-term safety analysis for deep geological repositories that use cement based materials in its structures.

2. Materials and methods

Cement grout specimens were cast with the Portland cement CP II-Z-32 of the Brazilian Standard NBR 11578 (ABNT, 1997), equivalent to the CEM II B of European Standards (EN, 2000). It is a cement with pozzolan addition, to which were added a cement additive (Superflow 4000, Bauchemie), normalized sand and distilled water. The water/cement ratio was 0.50. The sand/cement ratio was 1.00 and the amount of each component to make 1 kg of grout is shown in Table 1.

The cement grout was cast in an aluminium tray and maintained in a high humidity environment (100% R.H.) during the curing process (for 7 days). After curing, cylindrical samples of 30 mm high and 25 mm diameter were taken from the grout and then cut in 2 mm - thick slices (specimens) to be irradiated or stored as reference samples. Fig. 1 shows images of the specimens used in the tests.

The specimens were then stored in a dry nitrogen environment and submitted to gamma irradiation until achieving the accumulated dose of 600 kGy, at the Multipurpose Irradiation Facility of IPEN-CNEN/SP. The control specimens were stored in a dry nitrogen environment.

After the irradiation, the specimens were analyzed by simultaneous X-Ray Diffraction and MicroTomography and later by Time-of-Flight Spectrometry, in order to assess mineralogical changes induced by radiation. The X-Ray Diffraction and MicroTomography were done in the Energy Dispersive Diffraction beamline (EDDI) [19] of BESSY II synchrotron radiation source, at Helmholtz-Zentrum Berlin (HZB). The neutron Time-of-Flight Spectrometer NEAT [20] preliminary studies were done at BER II research reactor, at Helmholtz-Zentrum Berlin (HZB).

3. Results and discussion

3.1. X-ray diffraction

TOPAS software was used to refine the diffractograms obtained by X-Ray Diffraction analysis, using pre-determined phases. The phases used to refine the diffractograms were: tricalcium silicate (C_3S), dicalcium silicate (C_2S), Tetracalcium Aluminoferrite (C_4AF), Portlandite, Periclase, Quartz, Calcite, Ettringite and the CSH gel. Fig. 2 shows the refinement of diffractograms of non-irradiated (M – NI) and irradiated (M-IR) grout samples.

C_3S, C_2S and C_4AF are phases present in anhydrous cement, but that still remains after hydration. Quartz is the main phase of the sand and all other phases are commonly present in the hydrated cement.

The Rietveld refinement is a technique used to characterize crystalline materials and to refine a theoretical profile (in mono or multiphase systems) until the expected profile matches with the measured profile. The theoretical profile is calculated using information provided by the users about the phases that are present in the sample. To identify the samples, a “Search and Match” method was done using PanAlytical HighScore Plus software. This method searches the peaks in the measured profile (diffractograms) and matches them with known phases previously measured.

TOPAS refinement gives a series of parameters to verify if the calculated and measured profiles are matching. One of the parameters is the goodness of fitness (gof), which is the ratio between the weighted-profile (Rwp) and the expected-profile (Rexp). The gof ideal number is one. For multi-phases systems, the gof can be much higher. For cementitious materials, which have a large number of phases, a gof about five is considered acceptable.

Table 2 below shows the results of XRD for the specimens that were kept in dry storage and those irradiated for 4 weeks, both kept in a nitrogen atmosphere, to avoid calcite formation in the surface. “NI” samples are not irradiated and “IR” samples are the irradiated ones. The results are normalized to the quartz content that was 44.99% and 27.92% to the grout not irradiated sample (M – NI) and grout irradiated sample (M-IR), respectively.

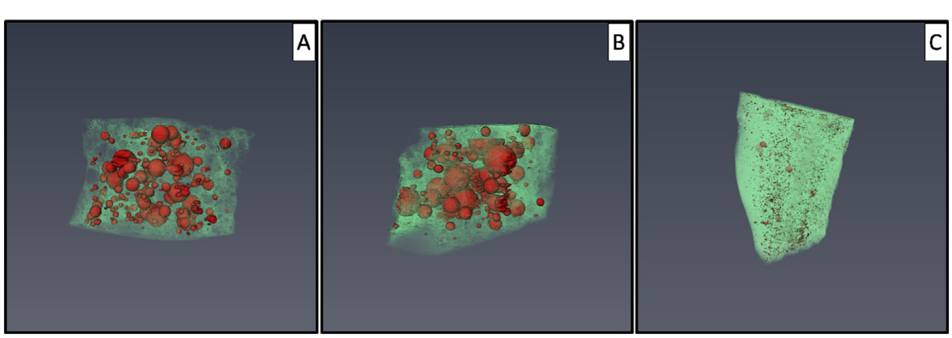

Fig. 4. An XY axis images for M-NI(A); M-IR(B); and CP samples(C).

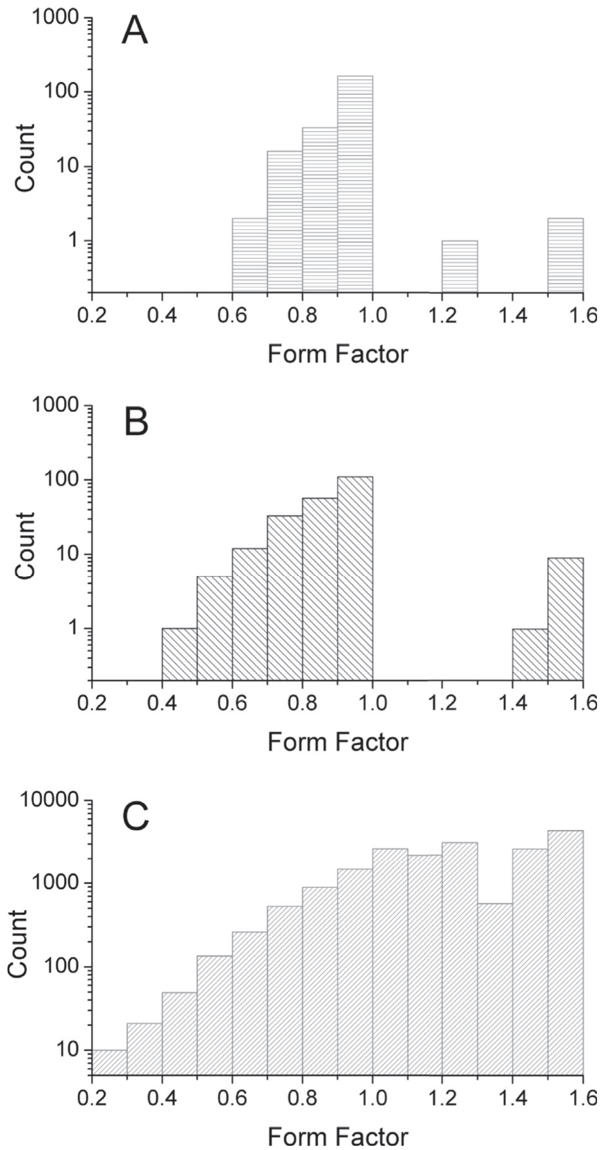

Fig. 5. Form factor of M – NI (A), M-IR (B) and CP (C).

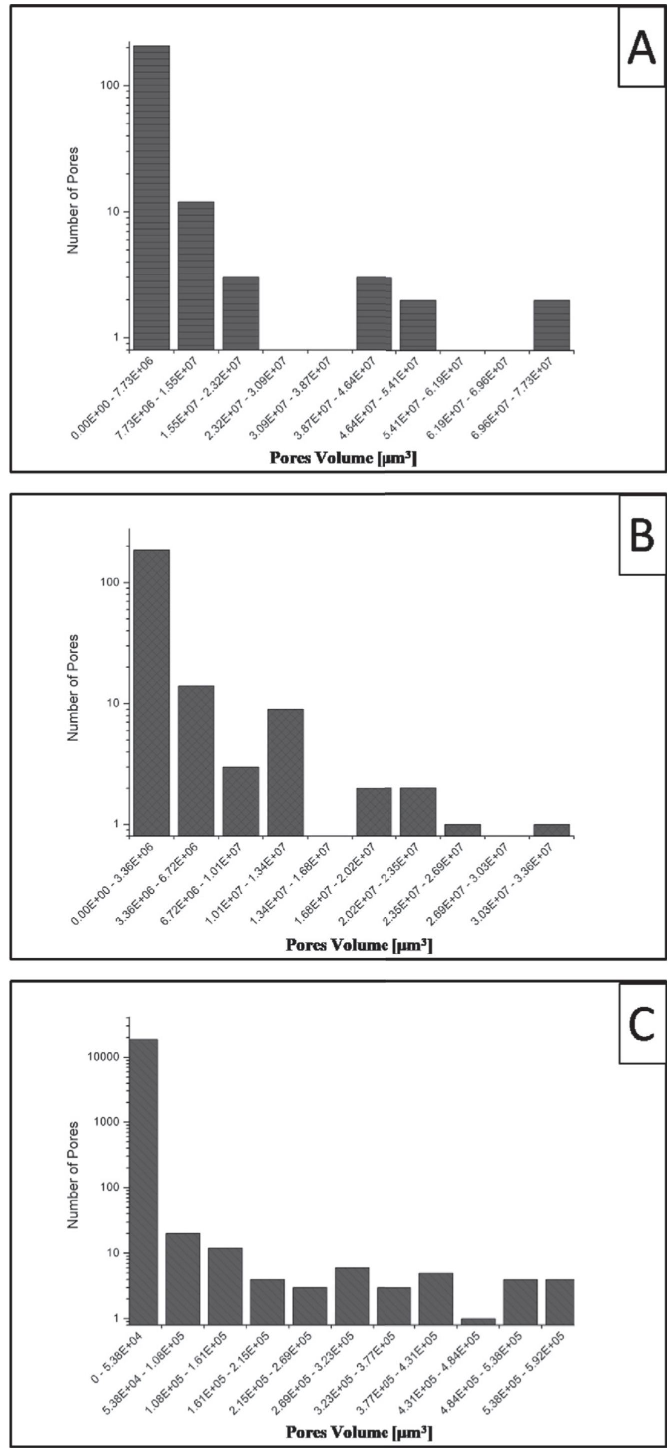

Fig. 6. Pore volume distribution of M – NI (A), M-IR (B) and CP (C).

Fig. 3 shows the difference between the samples as a function of the phases percentage. The comparison between them shows clearly the absence of ettringite in the sample that was submitted to irradiation.

It was possible to observe that irradiation causes microstructural changes in the cement grout. The ettringite depletion and an increase in C—S—H and Portlandite content, as well a decrease in anhydrous phases (Alite + Belite) were the most pronounced phases changes due to irradiation. Fig. 3 shows that the non-irradiated sample shows the presence of Ettringite (AFt), which has not been observed in the irradiated sample, suggesting that all AFt reacted with the aluminate compounds still present, favoring the formation of the AFm phase (monosulfate of low crystallization). These results are evidence that irradiation caused water radiolysis, a process which water is decomposed in primary species, as H_2, H_2O_2, OH^-, H_3O^+, and radicals. These species react with water to form secondary species [13]. All these species formed during radiolysis react with hydrated cement compounds.

Also, the irradiation can heat the material and increase internal temperature, causing the breakdown of chemical bonds, providing the formation of reactive species and thus favouring some types of reactions. This phenomenon provoked by radiation promote increase cement hydration degree [15].

The processes of decomposition and reformation of compounds catalyzed by radiation and radiolysis lead to ettringite depletion, which releases ions as sulfate and aluminate, and formation of Portlandite and C—S—H gel, as well other AFm phases as C2AH8 and C4AH13.

Results obtained by X-ray diffraction confirmed that content of these compounds was also increased by hydration degree, which was higher in irradiated samples, showing a lower alite and belite content in the irradiated sample.

3.2. Micro tomography

The micro tomography analysis shows that is possible to observe

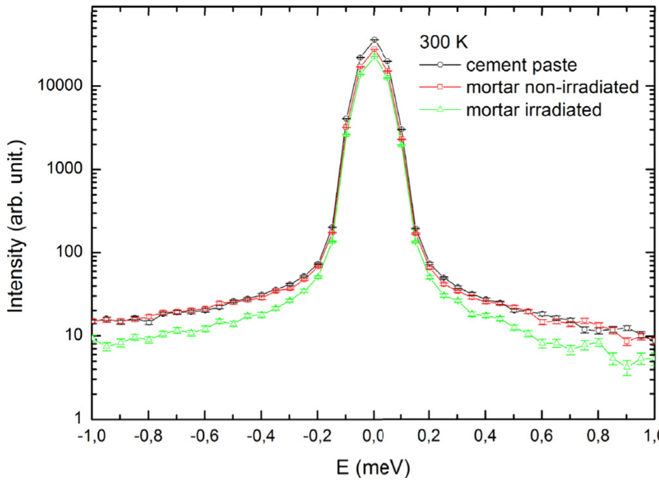

Fig. 7. Quasielastic neutron scattering spectra measured at 300 K.

differences in the porous of different specimens. The sample that was irradiated showed almost 8% of volumetric porosity, which is about 30% (M – NI) more than the grout sample that was not irradiated. This shows that the increase of the porosity is closely related to the effects provoked by irradiation. For illustrative purposes, we introduce the cement paste sample (water/cement ratio = 0.50) to analyze the effect of addiction of sand in the system.

The results show a significant difference between the grout and cement paste samples. Grout samples show a much higher total volumetric porosity than the cement paste sample. Comparing to the cement paste, the volumetric porosity of irradiated grout was almost 10 times higher. The pore volumes and fractions in each sample was showed in Table 3.

Fig. 4 shows the reconstructed 3D image for each sample. It is possible to observe that there more pores in the cement grout samples than in the cement paste specimen. The grout submitted to irradiation shows irregular pores, which can be caused by cracking during the tests.

The grout samples show large pores in its structure, probably due to the rim presence of sand and the superplasticizer, which probably increased the pore numbers and the pore radius.

Another essential property analyzed was Shape Factor of the pores which take into account the surface area of voids and the area of the smaller cross-section that passes through the center of mass.

$$\text{Form Factor} = \frac{(\text{surface area})^3}{36 \cdot \pi \cdot (\text{cross} - \text{section area})^2}$$

This parameter equals 1 when a pore has a spherical shape. As this factor differentiates from 1, the shapes of the pore approach to an ellipsoid [27].

Fig. 5 showed the distribution of the Form Factor versus the number of porous. It can be noted that M-IR sample presents porous with prevalence spherical which suggest that there are air bubbles inside the material. On another hand, cement paste sample has a greater number of pores than the other samples and an equitable distribution of the Form Factor. This can occur due to the better densification in this sample, which comprises the pores, changing its Form Factor.

CP samples showed micropores that suggest the observation of microstructure around the aggregate particles. This zone around the aggregate, called the interfacial transition zone (ITZ), is responsible for 99% (Fig. 6c) of the microporous observed in the CP sample.

Fig. 6 shows the similarity in the behavior of the pore volume distribution curves of sample M – NI and M-IR. It presented a higher number of smaller pores, gradually increasing until reaching the band from 2.02 10^7 to 2.35 10^7 μm^3 and 6.96 10^7 to 7.73 10^7 μm^3, respectively. The histograms obtained from the reconstruction of the images

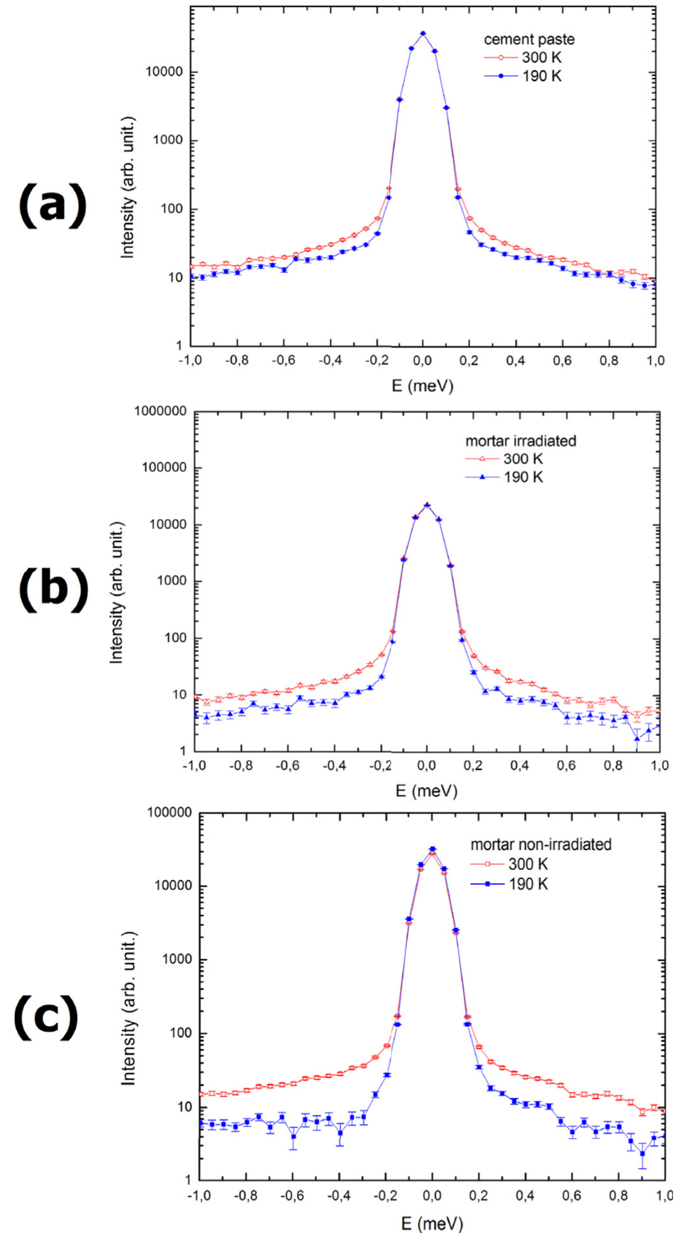

Fig. 8. Quasielastic neutron scattering spectra from the CP samples(a); M-IR (b) and M – NI (c) at measured temperature 300 K and 190 K.

showed that the M – NI and M-IR do not present pores in the range observed in CP sample. This result could also be observed visually by images showed in Fig. 4.

3.3. Quasielastic

Measurements performed by the quasielastic neutron scattering technique were also carried out to investigate the influence of radiation on cement samples and the changes caused by them. Preliminaries results obtained on irradiated, non-irradiated and paste samples showed differences that corroborate the results obtained by X-ray diffraction and tomography.

The results obtained at room temperature are shown in Fig. 7. We observed that section quasi-elastic (base of the curve) the irradiated sample presented a lower contribution of the confined water when compared to the others. This result shows that there was radiolysis and ratified the results obtained by X-ray diffraction, when we observed the increase of CSH, suppression of ettringite and increase of the amount of portlandite in the irradiated sample.

Our approach to validate the existence of confined water involved the realization of measurements at a temperature of 190 K. At this temperature we guarantee the crystallization of the confined water (which occurred from 210 K [21–26]), thus allowing to study its behavior.

Notice in Fig. 8 that the quasielastic signal decreases dramatically, this suggests that all water becomes crystalline, decreasing the quasielastic signal. Fig. 8a shows the results obtained at 300 and 190 K. It can be observed that the curves present non-significant difference, as obtained in sample 8b. This fact revealed that CP sample has less water (confined and free) than M-IR or M-NI. According to tomography measurements, this result is can be explained by the smaller amount of pores in the pastes relative to the non-irradiated sample. On the other hand, the non-significant difference between the 300 and 190 K curves in the irradiated samples is justified by the radiolysis, which decreases the amount of confined water when comparing the non-irradiated sample.

Unlike previous, Fig. 8c shows that the measurements performed at 300 and 190 K present a significant difference when compared with the others. This result shows that these samples have a greater amount of confined water.

These results that are not accessible by other techniques prove that differences in the amount of confined water in the cement samples can be observed. Further analysis still needs to be performed in order to get an actual modelling for the water dynamics in these complex systems.

4. Conclusions

The current study compares cement grout and cement paste samples with or without irradiation. It was possible to observe that the recipe of the grout used in this work increase substantially the larger size pores of the material when compared with cement paste.

Direct evidence acquired as decreasing the anhydrous phases of the cement and increasing Portlandite and C—S—H gel content, showed that irradiation provoked changes the mineralogy and microstructure of the samples. In addition, the irradiation causes a coarsening of the pores.

It is important to point that the irradiation dose used in this work was much lower than the accumulated doses that can be achieved in an intermediate and high-level waste repository. Nevertheless, at this dose, it was possible to observe significant changes in cement matrix and experiments with higher doses can lead to important deleterious effects in a cementitious matrix.

References

[1] E. Adamopoulou, P. Pipilikaki, M.S. Katsiotis, M. Chaniotakis, M. Katsioti, How sulfates and increased temperature affect delayed ettringite formation (DEF) in white cement mortars, Construct. Build. Mater. 25 (2011) 3583–3590, https://doi.org/10.1016/j.conbuildmat. 2011.03.051.

[2] J.W. Bullard, B. Lothenbach, P.E. Stutzman, K.A. Snyder, Coupling thermodynamics and digital image models to simulate hydration and microstructure development of portland cement pastes, J. Mater. Res. 26 (2011) 609–622, https://doi.org/10.1557/jmr.2010.41.

[3] F. Deby, M. Carcassès, A. Sellier, Probabilistic approach for durability design of reinforced concrete in marine environment, Cem. Concr. Res. 39 (2009) 466–471, https://doi.org/10.1016/j.cemconres.2009.03.003.

[4] R. Kaminskas, I. Barauskas, Influence of carbonated additives on Portland cement hydration in chloride environment, Adv. Cem. Res. 24 (2012) 365–372, https://doi.org/10.1680/adcr.11.00059.

[5] R. Loser, B. Lothenbach, A. Leemann, M. Tuchschmid, Chloride resistance of concrete and its binding capacity – comparison between experimental results and thermodynamic modeling, Cem. Concr. Compos. 32 (2010) 34–42, https://doi.org/10.1016/j.cemconcomp.2009.08.001.

[6] B. Lothenbach, B. Bary, P. Le Bescop, T. Schmidt, N. Leterrier, Sulfate ingress in Portland cement, Cem. Concr. Res. 40 (2010) 1211–1225, https://doi.org/10.1016/j.cemconres.2010.04.004.

[7] N. Ukrainczyk, N. Vrbos, J. Šipušić, Influence of metal chloride salts on calcium aluminate cement hydration, Adv. Cem. Res. 24 (2012) 249–262, https://doi.org/10.1680/adcr.11.00012.

[8] X. Cheng, S. Wang, L. Lu, Temperature capacitance effect of carbon fibre sulfoaluminate cement composite, Adv. Cem. Res. 24 (2012) 313–318, https://doi.org/10.1680/adcr.10.00068.

[9] D. Damidot, B. Lothenbach, D. Herfort, F.P. Glasser, Thermodynamics and cement science, Cem. Concr. Res. 41 (2011) 679–695, https://doi.org/10.1016/j.cemconres.2011.03.018.

[10] G. Le Saoût, E. Lécolier, A. Rivereau, H. Zanni, Chemical structure of cement aged at normal and elevated temperatures and pressures, Part II: low permeability class G oilwell cement, Cem. Concr. Res. 36 (2006) 428–433, https://doi.org/10.1016/j.cemconres.2005.11.005.

[11] B. Lothenbach, T. Matschei, G. Möschner, F.P. Glasser, Thermodynamic modelling of the effect of temperature on the hydration and porosity of Portland cement, Cem. Concr. Res. 38 (2008) 1–18, https://doi.org/10.1016/j.cemconres.2007.08.017.

[12] P. Bouniol, The influence of iron on water radiolysis in cement-based materials, J. Nucl. Mater. 403 (2010) 167–183, https://doi.org/10.1016/j.jnucmat.2010.06.020.

[13] P. Bouniol, E. Bjergbakke, A comprehensive model to describe radiolytic processes in cement medium, J. Nucl. Mater. 372 (2008) 1–15, https://doi.org/10.1016/j.jnucmat.2006.10.004.

[14] J.L. García Calvo, A. Hidalgo, C. Alonso, L. Fernández Luco, Development of low-pH cementitious materials for HLRW repositories: resistance against ground waters aggression, Cem. Concr. Res. 40 (2010) 1290–1297, https://doi.org/10.1016/j.cemconres.2009.11.008.

[15] I. Maruyama, O. Kontani, A. Ishizawa, M. Takizawa, O. Sato, Development of system for evaluating concrete strength deterioration due to radiation and resultant heat, in: Presented at the International Conference on Nuclear Power Plant Life Management (PLiM) for Long Term Operations (LTO), 2012 (Salt Lake City, Utah, United States).

[16] NAGRA, Effects of Post-disposal Gas Generation in a Repository for Low- and Intermediate-level Waste Sited in the Opalinus Clay of Northern Switzerland (No. TR 08–07), National Cooperative for the Disposal of Radioactive Waste, Wettingen, 2008.

[17] F. Vodák, V. Vydra, K. Trtík, O. Kapičková, Effect of gamma irradiation on properties of hardened cement paste, Mater. Struct. 44 (2011) 101–107, https://doi.org/10.1617/s11527-010-9612-x.

[18] F. Vodák, K. Trtík, V. Sopko, O. Kapičková, P. Demo, Effect of γ-irradiation on strength of concrete for nuclear-safety structures, Cem. Concr. Res. 35 (2005) 1447–1451, https://doi.org/10.1016/j.cemconres.2004.10.016.

[19] F.G. Moreno, C. Jiménez, P.H. Kamm, M. Klaus, G. Wagener, J. Banhart, Ch Genzel, Qhite-beam X-ray radioscopy and tomography with simultaneous diffraction at the EDDI beamline, J. Synchrotron Radiat. 20 (2013) 809–810.

[20] G. Günther, M. Russina, Background optimization for the neutron time-of-flight spectrometer NEAT, Nucl. Instrum. Meth. Phys. Res. 828 (2016) 250–261, https://doi.org/10.1016/j.nima.2016.05.022.

[21] F. Ridi, P. Luciani, E. Fratini, P. Baglioni, Water Confined in Cement Pastes as a probe of cement microstructure evolution, J. Phys. Chem. B 113 (2009) 3080–3087.

[22] M.B. Pinson, E. Masoero, P.A. Bonnaud, H. Manzano, Qing i, S. Yip, J.J. Thomas, M.Z. Bazant, K.J.V. Vliet, H.M. Jennings, Hysteresis from multiscale porosity: modeling water sorption and shrinkage in cement paste, Phys. Rev. App. 3 (2015), 064009.

[23] P.A. Bonnaud, Q. Ji, B. Coasne, R.J.M. Pellenq, K.J. Van Vliet, Thermodynamics of water confined in porous calcium-silicate-hydrates, Langmuir 28 (2012) 11422–11432, https://doi.org/10.1021/la301738p.

[24] M. Bauchy, M.J. Abdolhosseini Qomi, F.J. Ulm, R.J.-M. Pellenq, Order and disorder in calcium-silicate-hydrate, J. Chem. Phys. 140 (2014), 214503.

[25] V.M. Florez, N.R. Fox, Structure of supercritically dried calcium silicate hydrates (C–S–H) and structural changes induced by weathering, J. Mater. Sci. 48 (2013) 5022–5028, https://doi.org/10.1007/s10853-013-7289-6.

[26] Zhou Yi, Pei-Na Deng, L-Li Zhang, Hua Li, Dynamic behaviors of water contained in calcium-silicate-hydrate gel at different temperatures studies by quasi-elastic scattering spectroscopy, Chin. Phys. B 25 (10) (2016), 106401, https://doi.org/10.1088/1674-1056/25/10/106401.

[27] E.G.A. Ferreira, F. Yokaichiya, M.S. Rodrigues, A.A. Isaac, N. Kardjilov, M.K.K.D. Franco, Assessment of Greener Cement by employing thermally treated sugarcane straw ashes, Construct. Build. Mater. 141 (2017) 346–352, https://doi.org/10.1016/j.conbuildmat.2017.03.022.